The Osmotic Pressure of Concentrated Protein Solutions: Effect of Concentration and pH in Saline Solutions of Bovine Serum Albumin

VINCENT L. VILKER,[1] CLARK K. COLTON, AND KENNETH A. SMITH

Department of Chemical Engineering, Massachusetts Institute of Technology, Cambridge, Massachusetts 02139

Received April 17, 1980; accepted July 18, 1980

Osmotic pressure measurements are reported as a function of bovine serum albumin (BSA) concentration in 0.15 *M* sodium chloride at pH 4.5, 5.4, and 7.4. The measured values increased markedly with increasing BSA concentration and with increasing pH (and therefore increasing macroion charge). At a concentration of 450 g/liter solution and a pH of 7.4, osmotic pressure was nearly five atmospheres, which is more than four times the value measured at the same concentration and a pH of 4.5 and about 30 times the value expected for an ideal solution. A semiempirical analytical expression was developed which gave good agreement between prediction and the experimental data of this and other studies. The data were also compared to the prediction of a three-term virial equation wherein the second and third virial coefficients were calculated by using McMillan–Mayer solution theory. The expression for the potential of mean force was obtained by comparing various contributions to the potential energy of interaction. The terms for electrostatic repulsion and dispersion attraction are the same as those used in the DLVO theory of colloid stability. The predicted curves are of the correct order of magnitude and follow the correct qualitative trend with pH, but they fail to display the strong pH-dependence of the data. The factors responsible for this deficiency are assessed and opportunities for developing a more realistic potential function are identified.

INTRODUCTION

When a protein solution is ultrafiltered by a membrane, a region of increased concentration of the retained solute develops near the membrane surface. The concentration at the surface can approach, or even attain, the solubility limit for the protein, and the driving force for hydraulic flow is reduced by the increased osmotic pressure difference across the membrane. This phenomenon of concentration polarization can thus greatly reduce the hydraulic flux as compared to that attainable with pure water. In order to obtain a fundamental understanding of protein ultrafiltration, data are required for the transport and osmotic pressure properties of these concentrated solutions.

In the past osmotic pressure measurements of protein solutions have generally been confined to the dilute range and have been taken primarily for the purpose of obtaining molecular weight and conformational data (1–3). In only a few instances (e.g., 4–8) have measurements been made up to moderate concentrations, nor are existing theoretical models of highly nonideal solution behavior suitable for à priori prediction at high concentration. The traditional approach is the Donnan membrane equilibrium model. Within this context, the exact multicomponent chemical potential treatment of Scatchard (4, 5) simply correlates data within the range for which it is available. The same is true for semiquantita-

[1] Author to whom correspondence should be sent. Chemical, Nuclear, and Thermal Engineering Department, University of California, Los Angeles, California 90024.

0021-9797/81/020548-19$02.00/0

tive interpretation of the osmotic virial coefficients of protein solutions in terms of excluded volume and attractive interaction effects (7). The most promising approach is the McMillan–Mayer solution theory (9) from which osmotic virial coefficients can be estimated in a manner analogous to those for the pressure of an imperfect gas. Hill (10, 11, 12) has applied this theory to charged colloid particles which exhibit double-layer repulsion, but no comparison with experimental data has heretofore been attempted.

In this paper we report osmotic pressure measurements for solutions of bovine serum albumin (BSA) at concentrations ranging from 84 up to 475 g/liter solution, in 0.15 *M* sodium chloride at pH 4.5, 5.4, and 7.4. The measurements were made with a static membrane osmometer built to withstand the several atmospheres of pressure generated by these solutions. The data are fit by a semi-empirical correlation suggested by Donnan theory that also gives good agreement with data from other studies. Lastly, the contributions to the potential energy of interaction between albumin molecules in solution are evaluated using physical properties available in the literature, and the resulting expression for the potential of mean force is used with the McMillan–Mayer theory to predict second and third osmotic virial coefficients. The poor agreement that results between predicted and measured osmotic pressure reflects the inadequacy of a three-term virial expansion at the higher protein concentrations examined, and it highlights the need for a better description of the potential of mean force than is currently available to describe the strong pH-dependence of the data.

MATERIALS AND METHODS

Albumin solution. Albumin solutions were prepared by mixing BSA crystals (Pentex grade recrystallized Cohn Fraction IV, cat. no. 81-001, Miles Laboratories, Kanakkee, Illinois) with 0.15 *M* NaCl made from distilled water and analytical grade NaCl. All prepartions included sodium azide (ca. 10 mg/liter) as an antibacterial agent. For concentrations above about 300 g/liter solution, BSA crystals and saline were added to 50-ml centrifuge tubes which were agitated by vigorous vortexing motion.

Albumin crystals were used as received. According to the manufacturer, the final steps before recrystallization were ion exchange, which ideally removed all micro-ions except H^+ and OH^-, followed by addition of NaOH to raise the pH to 5.2. The average chloride ion content was 3 mg/g protein. No special steps were taken to remove bound lipids. Cellulose acetate electrophoresis in this study indicated 100% albumin purity, and acrylamide gel electrophoresis showed 4–7 polymer bands, thereby indicating the presence of some albumin oligomers.

Solution pH measurements (±0.01 pH unit) were made with a saturated KCl glass electrode. Solution adjustment of pH was made by addition of nonbuffered 0.1 *N* NaOH or HCl. Vigorous vortex mixing was employed to ensure that local protein denaturation would not occur during acid or base addition. The solutions were not analyzed for sodium or chloride ion concentrations. Because of the large aliquots of 0.1 *N* NaOH or 0.1 *N* HCl which were added for pH adjustment, and the slight variability of Cl^- content of different lots of albumin crystals, the concentrations of Na^+ and Cl^- following pH adjustment were slightly different from the 0.15 *M* saline initially added. The maximum difference for the most concentrated solution is estimated to be about 0.03 *M*.

All albumin solutions were noncloudy, but occasionally small strands of apparently denatured protein were observed. For this reason, the final step before an experimental run was filtration through a 0.1-μm filter for albumin concentration up to 300 g/liter or a 0.3-μm filter for solutions of higher concentration.

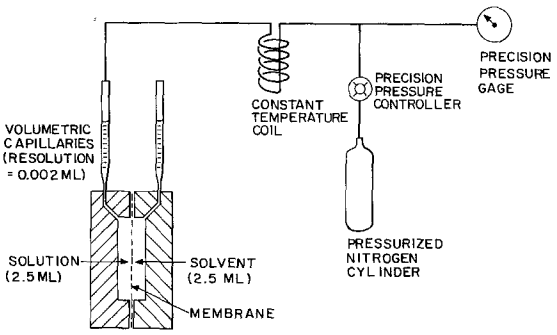

FIG. 1. Schematic diagram of high-pressure membrane osmometer system.

Albumin solutions charged to and discharged from the osmometer were analyzed for pH and for albumin concentration with the biuret method (13). The solution discharged from the solvent chamber was also routinely checked for possible albumin leakage with the biuret method or the Lowry method (14) which is more accurate when protein concentrations are very low. The precision of concentration measurement was ±5%.

Osmotic pressure measurement. The osmotic pressure measurement system is shown schematically in Fig. 1. The osmometer cell consists of two chambers, one for the 0.15 *M* saline solvent and one for the albumin solution. The chambers are separated by a membrane which is impermeable to albumin but permits free passage of water and microions. After the chambers are filled, a volumetric capillary prefilled with the appropriate solution is connected to each chamber. The gas pressure applied to the capillary on the solution chamber is then quickly set to the estimated osmotic pressure and subsequently adjusted in the direction indicated by slight movements in capillary liquid levels. Ultimately, an applied pressure is found for which liquid levels do not change over a period of several hours. This pressure is taken to be the solution colloid osmotic pressure. Applied pressure is measured and controlled to within several mm Hg by use of a precision pressure regulation gauge. The resolution of volume flow measurement by the volumetric capillaries is about 0.002 ml. The osmometer cell and gas temperature equilibration coil are immersed in a temperature bath controlled at 25 ± 0.1°C.

Figure 2 is a detailed view of the osmometer cell. The chambers are formed by sandwiching a membrane between two cylindrical pieces of Plexiglas, each of

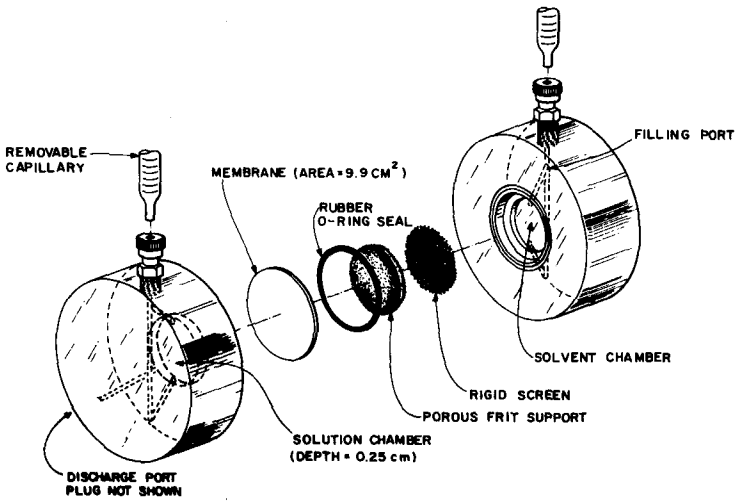

FIG. 2. Exploded view of the membrane osmometer cell.

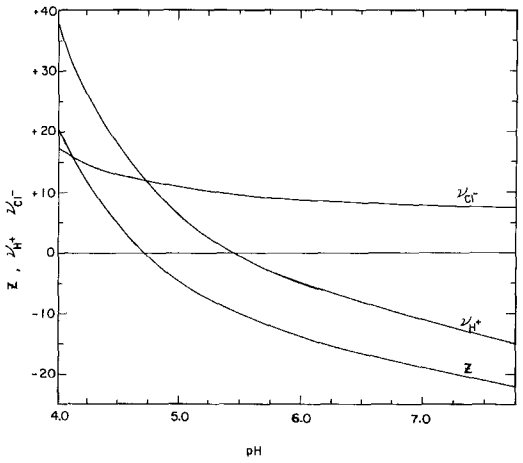

FIG. 3. Bovine serum albumin charge, Z, bound hydrogen ions, ν_{H^+}, and bound chloride ions, ν_{Cl^-} per albumin molecule in 0.15 M NaCl solution as a function of solution pH. Isoelectric pH = 4.72, isoionic pH = 5.46.

which contains a shallow circular depression (0.25 cm deep × 3.56 cm diameter). The membrane is supported on the solution side by a metal screen and a porous frit. One-eighth-in. diameter stainless-steel rods (not shown), equally spaced around the chambers about half-way to the outer perimeter, are used to clamp the unit together. A rubber O-ring impressed on the solvent side of the membrane seals the unit to applied pressures of at least 4500 mm Hg when the two halves are clamped. The cellulosic membranes (Abcor HFA-180 sheet stock) used for all determinations have a rejection coefficient of 0.99+ for albumin and not more than 2×10^{-4} for saline (15). Five membranes were used in the course of about 50 experimental measurements with no detectable differences in results for different membranes.

At the conclusion of each measurement, solvent and solution samples are taken with a syringe and needle via the filling ports. For concentrations of about 400 g/liter or more, rapid sample discharge was attained by removing the plug to the discharge port with the solution under pressure.

To confirm that stable liquid levels in the capillaries are indicative of true thermodynamic equilibrium, two separate determinations were made on identical starting solutions. In one, the initial applied pressure was less than the osmotic pressure of the solution; in the second it was greater. In each case, the applied pressure was adjusted until volume transfer between chambers ceased, and the two osmotic pressure measurements agreed to within about 4%. Additional details are available elsewhere (15).

Albumin valence calculation. For use in the models subsequently employed in this paper, the average net molecular charge of albumin is calculated from its complex equilibria with H^+ and Cl^- ions. In the pH range of our experiments, Na^+ binding is unimportant (16), and the availability of binding sites for H^+ and Cl^- is constant since there are no changes in the protein secondary structure (17). The macroion charge number Z is equal to the difference between the number of bound protons ν_{H^+} and the bound chloride ions ν_{Cl^-} per albumin molecule,

$$Z = \nu_{H^+} - \nu_{Cl^-}. \qquad [1]$$

The isoelectric pH ($Z = 0$) in 0.15 M saline solutions is about 4.72 (18, 19). The average albumin charge number is obtained by combining Tanford's proton binding data from titration measurements in 0.15 M NaCl (17) with the two-site chloride binding model of Scatchard *et al.* (20),

$$\nu_{Cl^-} = \frac{n_1 k_1 [Cl]\gamma \exp(2wZ)}{1 + k_1[Cl]\gamma \exp(2wZ)} + \frac{n_2 k_2 [Cl]\gamma \exp(2wZ)}{1 + k_2[Cl]\gamma \exp(2wZ)} \qquad [2]$$

where $n_1 = 10$, $k_1 = 44\ M^{-1}$, $n_2 = 30$, $k_2 = 1.1\ M^{-1}$, and [Cl] is the free chloride ion concentration in solution, 0.15 M. The parameters γ and w are calculated for our conditions to be 0.78 and 0.026, respectively (15). For a given pH, ν_{H^+} is found from Tanford's titration data as shown in Fig. 3,

and iterative calculation is then used to solve Eqs. [1] and [2] simultaneously for the values of ν_{Cl^-} and Z. These results are also shown in Fig. 3.

The isoionic pH ($\nu_{H^+} = 0$ by definition), measured following addition of BSA (50 g/liter) to 0.15 *M* NaCl, ranged from 5.22 to 5.55 pH for the various lots of albumin used in this work. These values are in good agreement with 5.46 pH as given by Tanford (17).

EXPERIMENTAL RESULTS

The albumin concentration C_p and pH measured in the solution discharged from the osmometer, the calculated albumin charge number, and the measured osmotic pressure are tabulated in Table I. The discharge concentration varied from the initial concentration by ±10% at most, and the pH of the discharged solution was never significantly different (±0.05 pH units) from its initial value. The albumin concentration in the solvent chamber discharge was usually 1 to 3 g/liter. These low concentrations did not contribute significant corrections to the reported osmotic pressures. From tests for thermodynamic equilibrium, the precision of osmotic pressure measurements was estimated to be within ±5%.

Reduced osmotic pressure π/C_p is plotted in Fig. 4 as a function of albumin concentration. The data at the lowest concentration for each pH are consistent with extrapolation to a value for the intercept, RT/M_p = 0.270 mm Hg/g/liter solution, which corresponds to the molecular weight of 69,000 first determined by Scatchard (5). This value is higher than that for monomeric albumin determined by amino acid sequencing, 66,100 (21), and it could result from the presence of about 5% dimers or higher oligomers. The osmotic pressure exhibits a strong dependence on albumin concentration and solution pH. At all values of pH, the slope at low concentration, and consequently the second virial coefficient, is positive. The nonlinear increase in π/C_p with increasing C_p indicates that the third term of the virial expansion makes a significant contribution to the osmotic pressure at all but the lowest concentrations studied. At the highest concentration examined, the osmotic pressure (about 5 atm) of the pH 7.4 solution is about five times larger than that of the pH 4.5 solution and about 30 times larger than the value predicted for an ideal solution by the van't Hoff equation.

In order to describe these results by an analytical expression, we fit the albumin osmotic pressure data to the following semi-

TABLE I

Osmotic Pressure of Bovine Serum Albumin Solutions

Albumin concentration, C_p (g/liter solution)	Solution pH	Albumin charge, Z	Osmotic pressure, π (mm Hg)
84	7.35	−20.2	48
91	7.37	−20.3	59
211	7.40	−20.4	332
211	7.46	−20.6	334
289	7.48	−20.7	844
325	7.34	−20.2	996
325	7.38	−20.3	996
354	7.40	−20.4	1423
357	7.50	−20.8	1638
413	7.44	−20.6	2620
428	7.44	−20.6	2806
448	7.42	−20.5	3640
91	5.41	−9.2	41
130	5.40	−9.1	74
144	5.40	−9.1	90
234	5.44	−9.5	260
240	5.45	−9.6	229
245	5.42	−9.3	269
338	5.40	−9.1	618
395	5.42	−9.3	1005
411	5.44	−9.5	1230
414	5.42	−9.3	1286
430	5.41	−9.2	1370
454	5.45	−9.6	1529
126	4.46	+5.5	47
182	4.54	+3.6	93
278	4.52	+4.1	182
317	4.50	+4.5	228
318	4.50	+4.5	244
343	4.52	+4.1	284
418	4.57	+3.2	716
475	4.50	+4.5	889

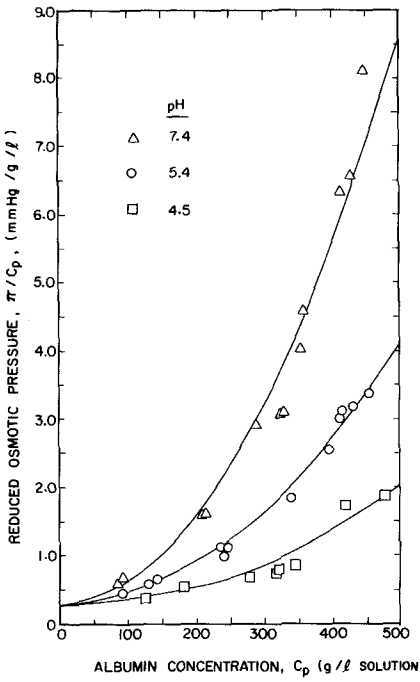

FIG. 4. BSA reduced osmotic pressure as a function of albumin concentration at 25°C and in 0.15 *M* NaCl at pH 7.4, 5.4, and 4.5. Curves are derived from Eqs. [3] to [5].

empirical function of albumin concentration:

$$\pi = RT\left\{2\left[\left(\frac{ZC_p}{2M_p}\right)^2 + m_s^2\right]^{1/2} - 2m_s\right\} + \frac{RT}{M_p}[C_p + A_2C_p^2 + A_3C_p^3] \quad [3]$$

where M_p is protein molecular weight, m_s is molar salt concentration, and C_p is albumin concentration (g/liter solution). The first term (in braces) accounts for the ideal Donnan effect, and the second term accounts for nonidealities arising from interactions of albumin macroions, microions, and water between themselves and each other. This approach was suggested by previous treatments based upon Donnan Theory (4, 5, 22, 23). We have further expressed the second term in the form of a virial expansion, the first term of which is the ideal van't Hoff contribution, and have taken the coefficients of the second and third terms to be quadratic functions of charge. A_2 and A_3 were evaluated by nonlinear least-squares regression analysis to yield

$$A_2 = -5.625 \times 10^{-4} - 2.410 \times 10^{-4} Z - 3.664 \times 10^{-5} Z^2 \quad [4]$$

$$A_3 = 2.950 \times 10^{-5} - 1.051 \times 10^{-6} Z + 1.762 \times 10^{-7} Z^2. \quad [5]$$

The prediction of Eqs. [3] to [5] is shown by the curves in Fig. 4 which give a good fit to the experimental data.

In Fig. 5 the semiempirical correlation is compared with osmotic pressure data for low and moderate albumin concentrations from Scatchard *et al.* (5) and Kappos and Pauly (8). The correlation predicts slightly higher values than those measured at 6.3 pH

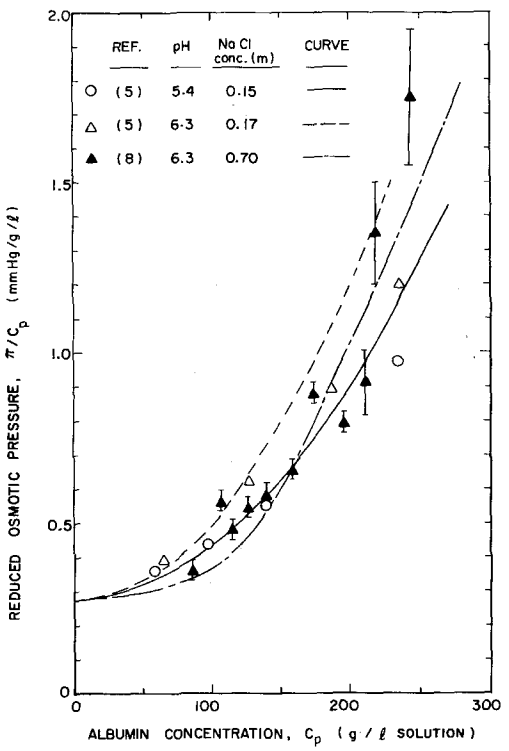

FIG. 5. Comparison of BSA osmotic pressure data from other studies with curves predicted by semi-empirical correlations of Eqs. [3] to [5].

and 0.17 *M* NaCl. Otherwise, the agreement with these other studies is excellent.

THEORY

Following the development of Hill (10–12), we consider a system in which the chemical potentials of water and microions are equal in both solutions, while albumin is present on only one side of the semipermeable membrane. The osmotic pressure can be equated to a virial expansion in powers of the solute number density.

$$\frac{\pi}{kT} = c + B_2c^2 + B_3c^3 + \cdots \qquad [6]$$

where the virial coefficients B_n have dimensions $(\text{cm}^3/\text{molecule})^{n-1}$. The solute number density is related to the weight concentration by

$$c = \frac{N_A C_p}{10^3 M_p}. \qquad [7]$$

According to McMillan–Mayer theory (9), the virial coefficients can be expressed in terms of cluster integrals and the function

$$f_{ij} = \exp[-W_{ij}/kT] - 1 \qquad [8]$$

where W_{ij} (subsequently denoted by W) is the potential of average force between solute (albumin) pairs i and j in an infinitely dilute solution ($c \to 0$) with center-to-center separation $\mathbf{r}_{ij}$ which we approximate by the intermolecular potential function. If the potentials are spherically symmetric, the first two coefficients in Eq. [6] are given by

$$B_2 = -\frac{1}{2V}\int_V\int_V f_{12}d\mathbf{r}_1d\mathbf{r}_2 = -2\pi\int_0^\infty f_{12}r^2dr \qquad [9]$$

$$B_3 = -\frac{1}{3V}\int_V\int_V\int_V f_{12}f_{13}f_{23}d\mathbf{r}_1d\mathbf{r}_2d\mathbf{r}_3 = -\frac{4\pi}{3}\int_0^\infty C_2(r)f_{12}r^2dr \qquad [10]$$

where

$$C_2(r_{12}) = \int_V f_{13}f_{23}d\mathbf{r}_3. \qquad [11]$$

The B_3 triple integral is partitioned to the form of Eq. [10] as suggested by Barker and Henderson (24) in order to facilitate the numerical computation discussed later in this paper. The analogy inherent in this development between the two-component system of "solute in solvent" and that of "gas in vacuum" is valid for solutions in which intermolecular forces are of sufficiently short range to ensure convergence of the cluster integrals. This constraint is satisfied for dilute solutions of macroions which contain sufficient electrolyte to provide Debye-type screening of the coulombic interactions.

Intermolecular Interactions

In order to construct a pair potential function, various contributions to the interaction between albumin molecules in electrolyte solution are examined. Analytical expressions for these contributions applicable to a spherical molecule of radius a are summarized in Table II.

Each of the electrostatic interactions is expressed as a product

$$W = W^*\xi. \qquad [12]$$

W^* is the pair potential function for particles immersed in a medium of dielectric constant ϵ but without ionic double layers; it reduces to the expression for interaction between ions in a vacuum when $\epsilon = 1$ (26). The factor ξ is a number less than unity which accounts for the screening of these interactions by the particle double layers. Similar screening effects occur with the induction interactions, but screening factors for these cases are not available in the literature. The W^* expressions for charge–dipole, dipole–dipole, and dipole-induced dipole interactions are the effective spherically symmetric potential functions averaged

TABLE II

Contribution to the Intermolecular Potential Function

Type	Designation	Unscreened potential function, W^*	Screening factor, ξ	Reference
Electrostatic				
Charge–charge	$W^{q,q}$	$+\frac{(Ze)^2}{\epsilon r}$	$\frac{ge^{-\kappa(r-2a)}}{(1+\kappa a)^2}$	(25)
Charge–dipole	$W^{q,\mu}$	$-\frac{2}{3}\frac{(Ze)^2\mu^2}{\epsilon^2 kTr^4}$	$\left\{\frac{3(1+\kappa r)e^{-\kappa(r-2a)}}{(1+\kappa a)[2+2\kappa a+(\kappa a)^2+(1+\kappa a)\epsilon_s/\epsilon]}\right\}^2$	(26, 27)
Dipole–dipole	$W^{\mu,\mu}$	$-\frac{2}{3}\frac{\mu^4}{kT\epsilon^2 r^6}$	$\left\{\frac{3[2+2\kappa r+(\kappa r)^2]^2 e^{-\kappa(r-a)}}{2+2\kappa a+(\kappa a)^2+(1+\kappa a)\epsilon_s/\epsilon}\right\}^2$	(27, 28)
Charge fluctuation	$W^{\Delta q,\Delta q}$	$-\frac{\langle Z^2\rangle^2 e^4}{2\epsilon^2 kTr^2}$	$\frac{e^{-2\kappa(r-2a)}}{(1+2\kappa a)^2}$	(29)
Induction				
Charge-induced dipole	$W^{q,\alpha}$	$-\frac{(Ze)^2\alpha}{\epsilon^2 r^4}$	Unknown	(26)
Dipole-induced dipole	$W^{\mu,\alpha}$	$-\frac{2}{3}\frac{\mu^2\alpha}{\epsilon^2 r^6}$	Unknown	(28)
Dispersion	$W^{\alpha,\alpha}$	$-\frac{A}{6}\left[\frac{2}{s^2}+\frac{2}{s^2-4}+\ln\left(\frac{s^2-4}{s^2}\right)\right]$		(30, 31)
		where		
		$A=(A_p^{1/2}-A_s^{1/2})^2$		
		$A_i=\pi^2\left(\frac{\rho_i N_A}{M_i}\right)\frac{3}{4}h\,\nu_{0i}\alpha_i^2$	$(i=\mathrm{p,s})$	
		$s=r/a$		

over all orientations; all other contributions tabulated are orientation independent.

Within the domain of the molecule, $W_{ij} = \infty$. For otherwise noninteracting rigid spheres of radius a such that $W_{ij} = 0$ for $r > 2a$, Eqs. [9] to [11] reduce to (26)

$$B_2 = \frac{16\pi}{3}a^3 = 4v_m \qquad [13]$$

$$B_3 = \frac{5}{8}B_2^2 \qquad [14]$$

and higher order coefficients are given by

$$B_4 = 0.2869B_2^3 \qquad [14a]$$

$$B_5 = 0.115B_2^4. \qquad [14b]$$

Consequently, the virial coefficients are usually evaluated by beginning the integration of Eqs. [9] to [11] at $r = 2a$ and adding the result to the respective excluded volume contribution. The prolate ellipsoid of axial ratio $p = a/b$ is a better model of albumin, for which case the excluded volume contributions are given by (24)

$$B_2 = [v_m + R_1S_1] \qquad [15]$$

$$B_3 = \left[v_m^2 + 2(R_1S_1)v_m + \frac{1}{3}(R_1S_1)^2\right] \qquad [16]$$

where

$$R_1 = \frac{a}{2}\left[1 + \frac{1-\epsilon^2}{2\epsilon}\ln\frac{1+\epsilon}{1-\epsilon}\right] \qquad [17]$$

$$S_1 = 2\pi b^2\left[1 + \frac{\sin^{-1}\epsilon}{\epsilon(1-\epsilon)^{1/2}}\right] \qquad [18]$$

$$\epsilon^2 = 1 - \frac{1}{p^2}. \qquad [19]$$

The dispersion contribution $W^{\alpha,\alpha}$ between spherical particles was derived by Hamaker (30) by assuming pairwise additivity of the intermolecular interaction. Far from the particle surface ($s \gg 1$), and in the absence of an intervening solvent, the expression in Table II reduces to

$$W^{\alpha,\alpha} = \frac{3}{4}\frac{h\nu_{0p}\alpha_p^2}{r^6} \qquad [20]$$

which was derived by London (32) for the dispersion interaction between two point molecules *in vacuo*. The dispersion interaction is unaffected by ionic double layer screening because the correlation time of the electronic fluctuations between atoms is much smaller than the time for adjustment of ions in the double layer.

The contribution $W^{\Delta q,\Delta q}$ originally suggested by Kirkwood and Shumaker (29) arises from time correlation between fluctuations in charge and charge distribution associated with fluctuations in number and configuration of the protons bound to albumin.

Rigorous calculation of the repulsive charge–charge potential energy of interaction first requires numerical solution of the nonlinear Poisson–Boltzmann equation for the electrical potential distribution surrounding a single macroion (33–36). When the electrical potential ψ at the surface of a macroion is less than about 50 mV, and the Debye length κ^{-1} is greater than about one-fifth of the macroion radius (as is the case in this study), the description of the potential distribution in the double layer by the linearized Debye–Hückel equation is applicable, and the electrical potential is given by

$$\psi = \frac{Ze}{\epsilon r(1+\kappa a)} e^{-\kappa(r-a)} \qquad [21]$$

where κ is defined by

$$\kappa^2 = \frac{4\pi e^2}{\epsilon kT}\sum_i c_i Z_i^2 \qquad [22]$$

and c_i is the number density of the ith microion of charge number Z_i. The expression for $W^{q,q}$ in Table II is based upon these approximations and is the relation originally developed by Verwey and Overbeek (25). The parameter g in the screening factor is less than unity; its magnitude depends on κr and on the boundary condition employed, constant surface potential ψ_0, or constant surface charge density. For the ionic strength and pH applicable here, $g > 0.9$ under all conditions (25, Table XX), and its value was set equal to unity for numerical evaluation.

An additional repulsive contribution (not shown in Table II) is present at separations for which electron clouds begin to overlap and nuclei of surface atoms begin to repel each other. This contribution is approximated by $W \to \infty$, and it limits the separation between particle surfaces to some minimum value σ. The integrations of Eqs. [9] to [11] are thus begun at $r = 2a + \sigma$, and the contributions from the region $2a < r \leq 2a + \sigma$ are properly included within the excluded volume contributions.

The physical parameter estimates used for quantitative evaluation of the potential function are summarized in Table III. The hydrated density we measured (15) was independent of albumin concentration to 560 g/liter solution and agrees well with other data (1). Estimates of albumin size and shape vary widely in the literature (1, 37, 38, 42–44), with molecular volume ranging from 86,000 (42) to 200,000 Å^3 and aspect ratio a/b ranging from 1.0 (43) to 6.5 (1). The estimates of Wright and Thompson (37) from rotational diffusion measurements in low salt solutions at 7.6 pH were selected as being the most reliable and representative of recent estimates, and they were used for calculating equivalent sphere and prolate ellipsoid dimensions. The tabulated dipole

TABLE III

Parameters Used to Evaluate Potential Functions

Parameter	Value	Reference
Albumin		
Molecular weight, M_p	69,000	(5)
Hydrated density, ρ	1.34 g/cm^3	(15)
Molecular volume, v_m	128,000 Å^3	(37)
Equivalent spherical radius, a	31.3 Å	
Ellipsoid shape		(37)
Semimajor axis, θ_a	70.5 Å	
Semiminor axis, θ_b	20.8 Å	
Dipole moment, μ	380×10^{-18} esu-cm	(38)
Polarizability, α_p	5950 Å^3	(39)
Characteristic frequency, ν_{0p}	3.06×10^{15} sec^{-1}	(39)
Charge number, Z	−20.4 at 7.4 pH −9.1 at 5.4 pH +4.5 at 4.5 pH	Fig. 3
Root-mean square charge number fluctuation, $\langle Z^2 \rangle^{1/2}$	3.5	(40)
Solvent (water)		
Polarizability, α_s	1.48	(26)
Characteristic frequency, ν_{0s}	4.35×10^{15} sec^{-1}	(26)
Dielectric constant		
Bulk value, ϵ	78.3	(41)
Local value at macroion surface, ϵ_s	4	(27)
Calculated		
Debye length, κ^{-1}	7.8 Å	Eq. [22]
Albumin surface potential, ψ_0	−23.5 mV at 7.4 pH −10.5 mV at 5.4 pH +5.2 mV at 4.5 pH	Eq. [21]
Hamaker constants		
A_p	7.27×10^{-13} ergs	
A_s	5.25×10^{-13} ergs	
A	1.65×10^{-14} ergs	

moment was determined with albumin in salt-free isoionic solution (38), and albumin polarizability and characteristic frequency was determined by refractive index measurements in 0.15 M NaCl (39). The charge fluctuation was evaluated in salt-free isoionic solution (40). A value lower by a factor of more than three has also been reported (45). The Debye length calculated from Eq. [22] is for the 0.15 M NaCl ionic strength of our albumin solutions. Others (46) have found that albumin solution conductance measurements are better fit by double layer theory when the protein concentration is included as a 1:1 electrolyte in Eq. [22]. This protein concentration dependence, which would have reduced κ^{-1} to 5.7 Å at the highest concentration and albumin charge studied, was not included in our calculations. The estimated minimum surface separation is 3.0 Å which corresponds to the minimum separation between peptide chains in proteins (47).

Pair Potential Function and Osmotic Pressure Calculation

The various contributions to the unscreened ($\xi = 1$) pair potential energy of interaction from Table II are compared in

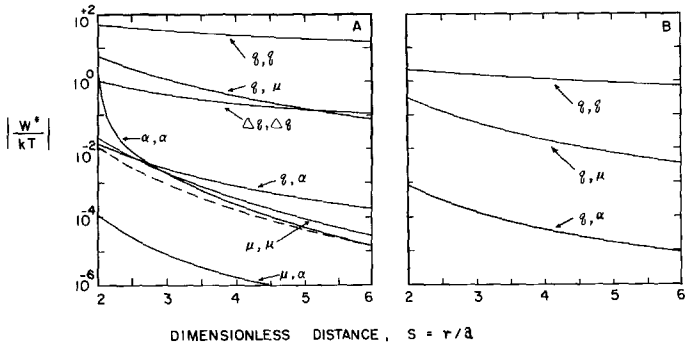

FIG. 6. Magnitude of unscreened pair potential energies of interaction for albumin as a function of center-to-center separation distance. Solid curves were calculated from equations in Table II. Dashed curve is from Eq. [20] for dispersion interaction between point albumin molecules, modified as in Table II to account for presence of intervening solvent. (A) pH 7.4; (B) pH 4.5.

Fig. 6. The potential energy is normalized by kT and center-to-center distance is normalized by the albumin equivalent spherical radius a. In the graph for pH 4.5 the same contributions which apply at pH 7.4 are present, but only those which depend on Z have been plotted. The largest contribution at each pH is the repulsive charge–charge interaction. Charge fluctuations and charge–dipole interactions are the most important attractive contributions, and the dispersion contribution calculated from the Hamaker equation is important only at very small separation.

Figure 7 is a similar plot which includes the effects of double layer screening on the electrostatic contributions. The magnitude of each of the electrostatic attractive components is substantially reduced. Although screening factors are not available for the induction contributions, the results in Fig. 6 provide no reason to expect that the screened induction contributions would be significant. The largest contributions are the repulsive charge–charge interactions and the attractive dispersion interactions. By ignoring the other contributions, the pair potential function becomes

$$W = W^{q,q} + W^{\alpha,\alpha}. \qquad [23]$$

The interplay between these two contributions forms the basis for the classical DLVO theory (25, 48) of colloid stability.

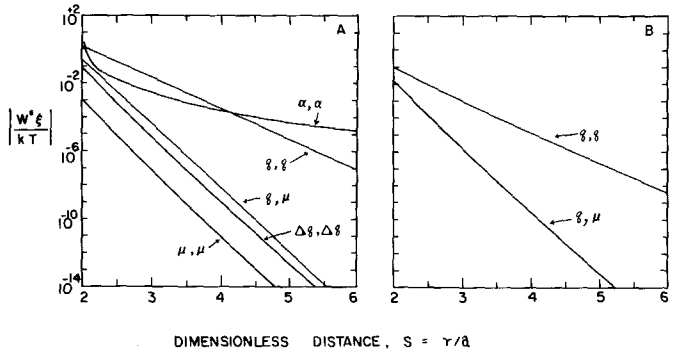

FIG. 7. Magnitude of screened-pair potential energies of interactions. (A) pH 7.4; (B) pH 4.5.

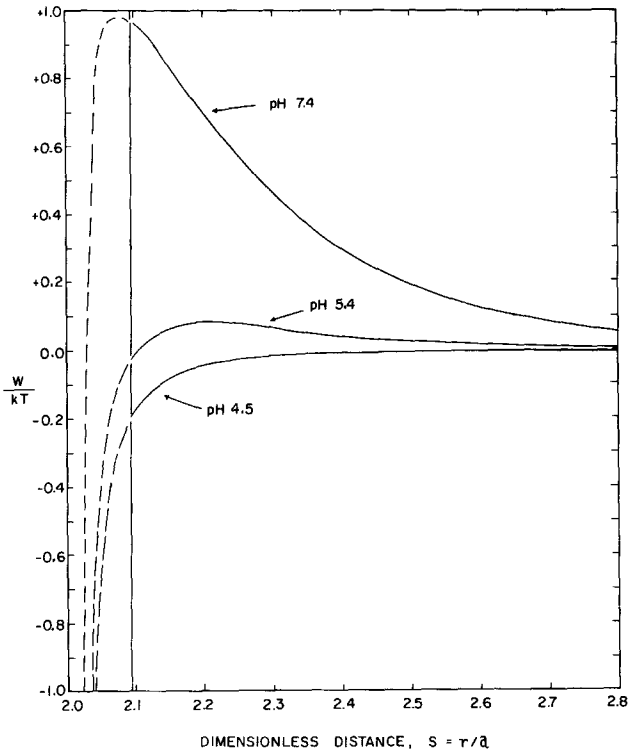

FIG. 8. Pair potential energy function calculated from Eq. [23] for pH 4.5, 5.4, and 7.4. Dashed curves show potential functions which would result if repulsive barrier at $s = 2 + \sigma/a$ were ignored.

The pair potential energy functions calculated from Eq. [23] are shown in Fig. 8. The variation with pH reflects the change in albumin charge (Fig. 3). Repulsion dominates at pH 7.4, and the maximum value of W/kT is about one. Repulsion dominates at pH 5.4 and attraction at pH 4.5, but in both cases the maximum absolute value of W/kT is only of order 10^{-1}. Not shown are local minima for pH 5.4 and 7.4 at $s \cong 4$ with $-W/kT = 0(10^{-4})$.

The osmotic pressure calculated from Eqs. [6] to [11] is the sum of the contributions from the excluded volume and from the region ($r > 2a + \sigma$) in which the potential function is finite. The effect of molecular size and shape on just the excluded volume contribution is shown in Fig. 9. The lower three curves are for a sphere with molecular volumes of 1.0 to 2.0 $\times$ 10^5 Å^3/molecule, a range which circumscribes most of the literature estimates. The upper two curves are for a prolate ellipsoid with v_m fixed at 1.50 $\times$ 10^5 Å^3/molecule and p = 3.2 or 4. Curve B, which lies between the data at pH 4.5 and 5.4, corresponds to the ellipsoid dimensions in Table II plus the repulsive contribution $\sigma/2$ (1.5 Å) added to each dimension so that v_m is effectively increased to 1.50 $\times$ 10^5 Å^3/molecule. The pH-dependence of the data could be explained, in part, by a shape change from sphere to prolate ellipsoid with increasing pH. Such a shape change between pH 4.5 and 5.4 has been suggested (43) but is not substantiated by more recent investigations (37, 38, 44).

The contribution from the region $r > 2a + \sigma$ was evaluated by numerical integration of Eqs. [9] and [10] using fourth-order Simpson's rule with the potential functions shown in Fig. 8. To evaluate B_3, the $C_2(r_{12})$

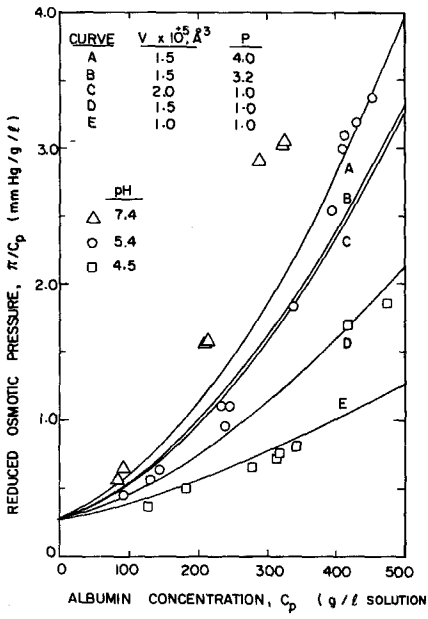

FIG. 9. Effect of molecular size and shape on calculated excluded volume contribution to reduced osmotic pressure as a function of albumin concentration. Data points are from Fig. 4.

integral was first rewritten in terms of the vector displacements from particle "1," $\mathbf{r} = \mathbf{r}_{12}$ and $\mathbf{r}' = \mathbf{r}_{13}$, to yield

$$C_2(\mathbf{r}) = \int_V f(\mathbf{r}')f(\mathbf{r}' - \mathbf{r})d\mathbf{r}'. \quad [24]$$

Repeated application of the one-dimensional convolution theorem then gives

$$\tilde{C}_2(\mathbf{k}) = \tilde{f}^2(\mathbf{k}) \quad [25]$$

where the tilde indicates the three-dimensional transform, that is $\tilde{f}(\mathbf{k})$ is the Fourier transform of the function f_{ij} defined by Eq. [8]. Since this function depends only on the magnitude r of the vector $\mathbf{r}$, its transform becomes similarly a function of the magnitude k alone. Then in spherical coordinates, the three-dimensional transform can be shown to reduce to a single integral (49).

$$\tilde{f}(k) = \frac{4\pi}{k}\int_0^\infty rf(r)\sin krdr \quad [26]$$

and the inverse transform of $\tilde{C}_2(k)$, denoted by F^{-1}, can similarly be shown to be

$$C_2(r) = \mathsf{F}^{-1}\{\tilde{C}_2(k)\} = \frac{1}{2\pi r^2}\int_0^\infty \{\tilde{f}^2(k)\}k\sin krdk. \quad [27]$$

Numerical algorithms similar to those of Lado (49) were used to solve Eqs. [26] and [27]. This solution for C_2 was used in Eq. [10].

The calculated estimates of B_2 and B_3 at each pH are tabulated in Table IV. These results are relatively insensitive to the value of σ over the range of 1.0 to 4.0 Å. At pH 4.5, B_2 is slightly decreased from the excluded volume contribution because the net pair potential function is attractive. However, the effect is small since $-W/kT$ is of the order of 10^{-1} (Fig. 8). B_2 increases from the excluded volume value for pH 5.4 and 7.4 at which the potential function is repulsive. B_3 is completely dominated by the excluded volume contribution and it is affected only at the fourth significant digit at the highest pH. Consequently, the ratio B_3/B_2^2 departs significantly from the excluded volume value. Reduced osmotic pressures calculated from the coefficients in Table IV are plotted in Fig. 10, and compared with the experimental data on Fig. 4. The qualitative trend of increasing osmotic pressure with increasing pH is consistent with the data, but quantitative agreement is poor because the predicted curves fail to show the great sensitivity of osmotic pressure to solution pH.

DISCUSSION

All measured osmotic pressures were greater than those which would be predicted for an ideal solution. The extent of nonideality increased to a remarkable extent with increasing BSA concentration and with increasing pH. The pH effect was presumably mediated by the increased absolute magnitude of the BSA net charge. The data

TABLE IV

Calculated Virial Coefficients

Contribution	B_2 (cm³/molecule)	B_3 (cm⁶/molecule²)	B_3/B_2^2
Excluded volume			
Sphere	5.999×10^{-19}	2.249×10^{-37}	0.625
Ellipsoid, $p = 3.2$	8.521×10^{-19}	3.974×10^{-37}	0.547
Incremental contribution from region of finite potential function			
pH 4.5	-0.119×10^{-19}	-7.8×10^{-45}	
pH 5.4	0.288×10^{-19}	5.5×10^{-43}	
pH 7.4	2.058×10^{-19}	1.1×10^{-40}	
Total (hard ellipsoid plus incremental contribution)			
pH 4.5	8.402×10^{-19}	3.974×10^{-37}	0.563
pH 5.4	8.809×10^{-19}	3.974×10^{-37}	0.512
pH 7.4	10.579×10^{-19}	3.976×10^{-37}	0.355

were fit well by a semiempirical relation, Eq. [3], which incorporated terms for the ideal Donnan effect and for solution nonidealities expressed as a function of net charge. Equation [3] also agreed well with data from other studies, and it should provide a good estimate of BSA osmotic pressure in 0.15 *M* NaCl solutions at any pH from 4.5 to 7.4. These results have been used in other studies on the ultrafiltration of BSA solutions (50, 51) which showed the predominant influence of BSA osmotic pressure at the membrane surface in determining volume flux.

We have attempted to describe the departure from ideal solution behavior with a three term virial equation by use of the McMillan–Mayer theory together with a priori evaluation of the principal contributions to the potential of mean force. The predicted osmotic pressures were of the correct order of magnitude and gave the correct qualitative trend with pH, but they lacked the strong dependence on pH displayed by the data. It is instructive to inquire as to which factors may be responsible for this lack of agreement.

A three-term virial equation may be insufficient for quantitative prediction. This is definitely true at the highest pH and albumin concentrations examined. For example, the ratio B_3C_p/B_2 calculated from the parameters in Table IV is about one at pH 7.4 and $C_p = 500$ g/liter solution, and a substantial

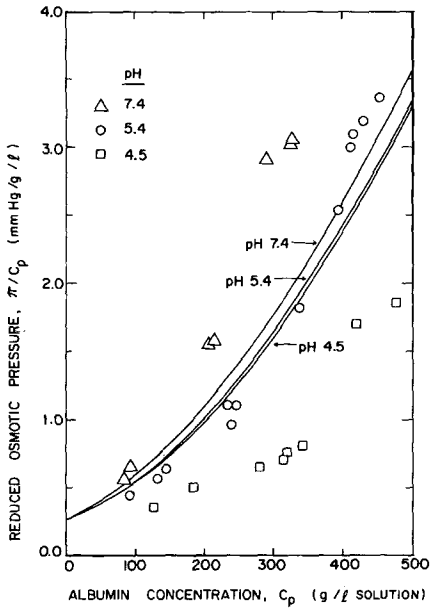

FIG. 10. Comparison between measured and predicted reduced osmotic pressure as a function of albumin concentration.

contribution from the fourth and higher terms is to be expected at such high concentration. That contributions beyond the third term make large contributions at this high concentration can be clearly seen through use of Eqs. [13] to [14b] for noninteracting rigid spheres. However, at the lower values of concentration and pH studied, the fourth and higher terms in the virial expansion should be negligible. The relative insensitivity of B_3 to pH further suggests that the use of only three terms in the equation is not the primary source for the small pH dependence of the predicted osmotic pressure, even in regions where the fourth term would be significant.

The excluded volume provided the major contribution to the estimated second and third virial coefficients (Table IV). A substantial change in size or shape with pH could explain the observed behavior in terms of excluded volume effects, but such changes are unlikely. The incremental contribution resulting from integration over the region $r \geq 2a + \sigma$ was small compared to the excluded volume contribution, even at pH 7.4, which accounts in part for the insensitivity to the magnitude of σ. The description of albumin as an ellipsoid rather than a sphere significantly increased the excluded volume contribution. If the potential function and Eqs. [9] to [11] were replaced by the appropriate orientation-dependent expressions for an ellipsoidal particle, the contribution from the region beyond the excluded volume would be similarly increased. Although the dependence of predicted osmotic pressure on pH would thereby be increased, it is unlikely that this change alone would provide a sensitivity comparable to that of the experimental data.

The arguments to this point suggest that the major defect in the analysis is in the description of the potential of mean force. The predicted curves in Fig. 10 are bracketed by the experimental data at the different values of pH studied. Agreement between theory and data therefore requires an increase in magnitude of both the repulsive (including excluded volume) and attractive contributions and an increased dependence on pH (or BSA charge) of one or both.

The data of this and other studies suggest that various attractive contributions may be substantially larger than we have estimated. For example, the data at pH 4.5 in Fig. 10 fall substantially below the predicted curve which means that the total magnitude of the attractive contributions is a substantial fraction of the excluded volume contribution plus whatever additional repulsive contributions exist at that pH. Because double layer screening is extensive in 0.15 *M* NaCl, it is reasonable to speculate that the attraction is dominated by dispersion forces. However, dipole moment fluctuation arising from proton fluctuations are thought to increase with decreasing pH (52) so that a large contribution from $W^{\Delta q,\Delta q}$ cannot be ruled out. Even larger attractive contributions which resulted in a negative value of B_2 were observed with BSA in isoionic salt-free solutions for which $Z \sim 0$ (53). This indicates the presence of a total attractive force which more than compensates for the effects of excluded volume and repulsion under conditions when double layer screening and average charge are negligible. Clearly, one or more of the unscreened contributions plotted in Fig. 6 must be very much larger than we have estimated.

The equations listed in Table II likely represent an overly simplistic picture of BSA intermolecular interactions. A number of deficiencies can be identified which may provide opportunities for improved representation of the potential of mean force:

(1) The equations for the electrostatic and induction contributions are strictly valid only at large distances from the molecule and become progressively less reliable as the surfaces approach. They are based on the assumption of a point charge and/or dipole embedded in the center of the mole-

cule. This can lead to substantial error, especially when the major contributions are confined to within several radii of the surface because of double layer screening. Just as the equation derived by Hamaker (30), which accounts for the finite size of the particle, predicts much greater interaction energy over this region than London's equation (32) for point molecules (Fig. 6), the actual electrostatic and induction contributions may be much greater than we estimate.

(2) We have assumed a uniform distribution of charge. The presence on different molecules of local fixed or fluctuating nonuniform but complementary constellations of surface charges (29, 54) could lead to preferred orientations between two BSA molecules and to increased electrostatic interactions.

(3) The correct value of the effective Hamaker constant A is uncertain. A variety of expressions have been derived for evaluating A_i between like materials (31). The equation in Table II, which is based upon London's original derivation, has proven reliable in other colloid applications (31) but its utility for such a large molecule as BSA is untested. There is also uncertainty in the expression used to account for the influence of the solvent medium on the dispersion interaction (28, 55). Srivastava (56) reported an experimentally determined Hamaker constant for albumin in water which was about 40 times the value we calculate. This is probably a large overestimate, since its use in our analysis leads to a large negative value for B_2, even at pH 7.4. Nonetheless, a substantial increase over our estimate is conceivable.

Our evaluation of attractive contributions to the potential of mean force is based on the so-called microscopic approach to van der Waals interactions between bodies (57). Some of the deficiencies cited above may be alleviated by use of Lifshitz macroscopic-continuum theory for interaction between condensed bodies (57–59) which may be a fruitful vehicle for further analysis. Because of its continuum character, it includes all many-body forces, retains contributions from all interaction frequencies, and treats correctly the effect of an intervening solvent medium. However, application of Lifshitz theory will require dielectric permeability data for albumin over the complete electromagnetic frequency spectrum at each of the pH values studied, and its use for a spherical polyelectrolyte surrounded by an ionic double layer has not yet been developed.

The repulsive contributions may also be larger and have greater charge dependence than we have estimated. Because the BSA surface charge results from proton association and dissociation reactions involving partially ionizable groups, the surface potential depends on a surface charge which is itself a function of potential through its dependence on the local pH and ionic strength. Analysis of this problem for cylindrical polyelectrolytes bearing a single type of ionizable group on the surface showed that surface charge and surface potential increase when the double layers overlap (60, 61). Incorporation of this effect would lead to larger estimates of $W^{q,q}$ than we calculated. Two other sources of repulsive forces which decay rapidly with distance from the surface have also been described: (a) a strong, exponentially varying force which is thought to result from the work of removal of waters of hydration around polar groups (62); and (b) a force which results from interaction of the gradient of dielectric constant near the surface of an ion immersed in water and the electric field generated by another ion and which adds to the potential function a contribution that is proportional to the square of the charge and to the local gradient in dielectric constant and falls off with separation as r^{-3} (63).

In the microscopic DLVO theory which we used, the various contributions to the potential energy are evaluated separately and added together, a procedure for which no firm basis is established from fundamental statistical mechanics. Barnes and

Davies (64) derived an alternate approach for obtaining the interaction energy of a system of charged bodies immersed in an electrolyte which extends Lifshitz theory to incorporate at once the interactions of overlapping double layers as well as dispersion forces between macroscopic bodies. They applied their theoretical result to the limited case of interaction between flat plates and for small surface charges so that the linearized Poisson–Boltzmann equation could be used for the electrostatic potential distribution. Most noteworthy in their results is the discovery of a new repulsion term (in addition to the usual repulsive electrostatic free energy) which is proportional to the square of the surface potential and which falls off with separation as $(\kappa r)^{-4}$. This additional term dominates the electrostatic repulsion at large separation since the electrostatic term falls off as $e^{-\kappa r}/\kappa r$. This theory is not currently available for evaluating the interaction energy between other geometrical shapes. However, the additional repulsive contribution found by Barnes and Davies may play an important role in the potential of mean force between BSA molecules and would be a fruitful subject for further research.

APPENDIX 1: NOTATION

A	Hamaker constant, ergs
a	Equivalent spherical radius, Å
B_n	Virial coefficients, $(cm^3/molecule)^{n-1}$
c	Number density, molecules/cm^3
C	Weight concentration, g/liter solution
C_2	Function defined by Eq. [11]
e	Electronic charge, 4.802×10^{-10} esu
f_{ij}	Function defined by Eq. [8]
g	Verwey–Overbeek correction to screened charge–charge interaction energy
h	Planck's constant, 6.627×10^{-27} erg × sec
k	Boltzmann's constant, 1.38×10^{-16} erg × K^{-1}
M	Molecular weight, g/g mole
N_A	Avogadro's number, 6.024×10^{23} molecules/g mole
p	Aspect ratio of ellipsoid
R	Gas constant, 62.36 mm Hg/(K × g mole/liter)
R_1	Ellipsoid geometry parameter defined by Eq. [17], Å
r_{ij}	Intermolecular center-to-center separation, Å
S_1	Ellipsoid geometry parameter defined by Eq. [18], Å
s	Dimensionless intermolecular separation, r/a
T	Absolute temperature, °K
v_m	Molecular volume, $Å^3$/molecule
W	Intermolecular potential between pairs of solute molecules, erg
Z	Macroion charge number
$\langle Z^2 \rangle^{1/2}$	Macroion root-mean square charge number fluctuation
α	Polarizability, $Å^3$
ϵ	Dielectric constant in free solution
ϵ_s	Dielectric constant for polarized water at macroion surface
$\theta_{a,b}$	Semiaxes of ellipsoid
κ	Debye screening parameter defined by Eq. [22], $Å^{-1}$
μ	Permanent dipole moment, esu × cm
ν_i	Number of bound microions i per macroion
ν_0	Characteristic frequency, sec^{-1}
ξ	Screening function
π	Colloid osmotic pressure, mm Hg
ρ	Density, g/cm^3
σ	Minimum separation between particle surfaces, Å
ψ	Electrostatic potential, volts

Superscripts

q	Net charge
Δq	Charge fluctuation
μ	Permanent dipole
α	Induced dipole

Subscripts

s Solvent
p Protein (albumin)

ACKNOWLEDGMENTS

This work was supported in part by NIH Grants No. HL 14209 and HL 21429. The authors gratefully acknowledge helpful conversations with J. Th. G. Overbeek, W. G. McMillan, and A. DiLeo.

REFERENCES

1. Tanford, C., "Physical Chemistry of Macromolecules." Wiley, New York, 1961.
2. Overton, J. R., *in* "Physical Methods of Chemistry, Part V" (A. Weissberger, Ed.), p. 309. Wiley-Interscience, New York, 1971.
3. Tombs, M. P., and Peacocke, A. R., "The Osmotic Pressure of Biological Macromolecules." Clarendon Press, London, 1974.
4. Scatchard, G., *J. Amer. Chem. Soc.* **68,** 2315 (1946).
5. Scatchard, G., Batchelder, A. C., Brown, A., and Zosa, M., *J. Amer. Chem. Soc.* **68,** 2610 (1946).
6. Shaw, M., *Biophys. J.* **16,** 43 (1976).
7. Chattorag, D. K., and Chatterjee, R., *J. Colloid Interfac. Sci.* **54,** 364 (1976).
8. Kappos, A. D., and Pauly, H., *Biophysik* **3,** 131 (1966).
9. McMillan, W. G., and Mayer, J. E., *J. Chem. Phys.* **13,** 276 (1945).
10. Stigter, D., and Hill, T. L., *J. Phys. Chem.* **63,** 55 (1959).
11. Hill, T. L., "Introduction to Statistical Thermodynamics," Ch. 19. Addison-Wesley, Reading, Massachusetts, 1960.
12. Hill, T. L., *Faraday Soc. Disc.* **21,** 31 (1956).
13. Henry, R. J., "Clinical Chemistry Principles and Techniques," p. 190, Harper and Row, New York, 1964.
14. Lowry, O. H., and Bessey, O. A., *J. Biol. Chem.* **163,** 633 (1946).
15. Vilker, V. L., Ph.D. Thesis, Massachusetts Institute of Technology, Cambridge, Massachusetts (1975).
16. Scatchard, G., and Black, E. S., *J. Phys. Colloid Chem.* **53,** 88 (1949).
17. Tanford, C., Swanson, S. A., and Shore, W. S., *J. Amer. Chem. Soc.* **77,** 6414 (1955).
18. Alberty, R. A., *J. Phys. Colloid Chem.* **53,** 114 (1949).
19. Longsworth, L. G., and Jacobsen, C. F., *J. Phys. Colloid Chem.* **53,** 126 (1949).
20. Scatchard, G., Scheinberg, I. H., and Armstrong, S. H., Jr., *J. Amer. Chem. Soc.* **72,** 535 (1950).
21. Brown, J. R., *in* "Albumin Structure, Function and Uses" (W. M. Rosenoer, M. Oratz, and M. A. Rothschild, Eds.), p. 1. Pergamon Press, New York, 1977.
22. Lauffer, M. A., *Biochemistry* **5,** 1952 (1966).
23. Rice, S. A., and Nagasawa, M., "Polyelectrolyte Solutions," p. 406. Academic Press, New York, 1961.
24. Barker, J. R., and Henderson, D., *Rev. Modern Phys.* **48,** 587 (1976).
25. Verwey, E. J. W., and Overbeek, J. Th. G., "Theory of the Stability of Lyophobic Colloids," p. 135. Elsevier, Amsterdam, 1948.
26. Hirschfelder, J. O., Curtiss, C. F., and Bird, R. B., "Molecular Theory of Gases and Liquids," Ch. 13, Wiley, New York, 1954.
27. Phillies, G. D. J., *J. Chem. Phys.* **60,** 2721 (1974).
28. Setlow, R. B., and Pollard, E. C., "Molecular Biophysics," Ch. 6. Addison-Wesley, Reading, Mass., 1962.
29. Kirkwood, J. G., and Shumaker, J. B., *Proc. Nat. Acad. Sci. USA* **38,** 863 (1952).
30. Hamaker, H. C., *Physica* **4,** 1058 (1937).
31. Visser, J., *Advan. Colloid Interface Sci.* **3,** 331 (1972).
32. London, F., *Trans. Faraday Soc.* **33,** 8 (1937).
33. Hoskin, N. E., *Trans. Faraday Soc.* **49,** 51 (1953).
34. Brenner, S. L., and Roberts, R. E., *J. Phys. Chem.* **77,** 2367 (1973).
35. Hoskin, N. E., and Levine, S., *Phil. Trans. Royal Soc. London* **A248,** 449 (1956).
36. Honig, E. P., and Mul, P. M., *J. Colloid Interface Sci.* **36,** 258 (1971).
37. Wright, A. K., and Thompson, M. R., *Biophys. J.* **15,** 137 (1975).
38. Squire, P. G., Moser, P., and O'Konski, C. T., *Biochemistry* **12,** 4261 (1968).
39. Andersen, M., Painter, L. R., and Nir, S., *Biopolymers* **13,** 1261 (1974).
40. Timasheff, S. N., Dintzis, H. M., Kirkwood, J. G., and Coleman, B. D., *J. Amer. Chem. Soc.* **79,** 782 (1957).
41. Robinson, R. A., and Stokes, R. H., "Electrolyte Solutions," 2nd ed., p. 457. Butterworths, London, 1959.
42. Soetewey, F., Roseneau-Motreff, M., Lamote, R., and Peeters, H., *J. Biochem.* **71,** 705 (1972).
43. Champagne, M., *J. Polym. Sci.* **23,** 863 (1957).
44. Wright, A. K., and Baxter, J. E., *Biophys. J.* **16,** 931 (1976).
45. Baskin, L. S., *J. Phys. Chem.* **72,** 2958 (1968).
46. Möller, W. J. H. M., van Os, G. A. J., and Overbeek, J. Th. G., *Trans. Faraday Soc.* **57,** 235 (1961).

47. Edsall, J. T., *in* "High Molecular Weight Organic Compounds" (R. E. Burk and O. Grummit, Eds.), p. 145. Interscience, New York, 1949.
48. Derjaguin, B., and Landau, L., *Acta Phys. USSR* **14,** 633 (1941).
49. Lado, F., *J. Comput. Phys.* **8,** 417 (1971).
50. Vilker, V. L., Colton, C. K., Smith, K. A., and Greene, D., Paper 1d, 77th American Institute of Chemical Engineers National Meeting, Pittsburgh, Penn. (1974).
51. Vilker, V. L., Colton, C. K., and Smith, K. A., *AIChE J.*, in press (1980).
52. Kirkwood, J. G., and Shumaker, J. B., *Proc. Nat. Acad. Sci. USA* **38,** 855 (1952).
53. Gutfreund, H., *Trans Faraday Soc.* **50,** 628 (1954).
54. Timasheff, S. N., *in* "Biological Polyelectrolytes" (A. Veis, Ed.), p. 1. Marcel Dekker, New York, 1970.
55. Kestner, N. R., and Sinanoglu, O., *Disc. Faraday Soc. London* **40,** 266 (1965).
56. Srivastava, S. N., *Z. Phys. Chem. (Liepzig)* **233,** 237 (1966).
57. Nir, S., *Progr. Surface Sci.* **8,** 1 (1976).
58. Parsegian, V. A., *Ann Rev. Biophys. Bioeng.* **2,** 221 (1973).
59. Mahanty, J., and Ninham, B. W., "Dispersion Forces." Academic Press, New York, 1976.
60. Brenner, S. L., and McQuarrie, D. A., *J. Colloid Interface Sci.* **44,** 298 (1973).
61. Brenner, S. A., and McQuarrie, D. A., *Biophys. J.* **13,** 301 (1973).
62. LeNeveu, D. M., Rand, R. P., Parsegian, V. A., and Gingell, D., *Biophys. J.* **18,** 209 (1977).
63. Bahe, L., *J. Phys. Chem.* **76,** 1062 (1972).
64. Barnes, C. J., and Davies, B., *J. Chem. Soc. Faraday Trans. II* **71,** 1667 (1975).